

# Metal-free Borylation of $\alpha$ -Naphthamides and Phenylacetic Acid Drug

Suman Maji, Parveen Rawal, Animesh Ghosh, Karishma Pidiyar, Shael A. Al-Thabaiti, Puneet Gupta,\* and Debabrata Maiti\*



Cite This: *JACS Au* 2024, 4, 3679–3689



Read Online

ACCESS |

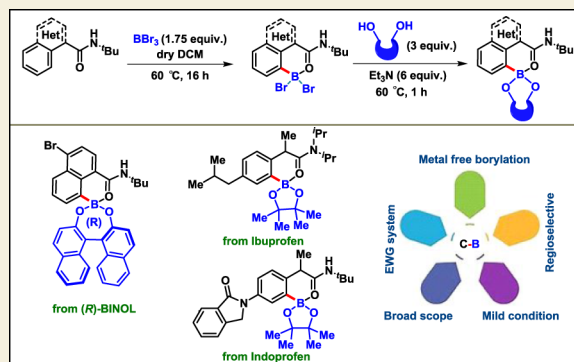
Metrics & More

Article Recommendations

Supporting Information

**ABSTRACT:** Site-selective C–H borylation is an important strategy for constructing molecular diversity in arenes and heteroarenes. Although transition-metal-catalyzed borylation is well explored, developing metal-free strategies remains scarce. Herein, we developed a straightforward approach for  $\text{BBr}_3$ -mediated selective C–H borylation of naphthamide and phenyl acetamide derivatives under metal-free conditions. This methodology appears to be economical and cost-effective. Successful borylation of drug molecules such as ibuprofen and indoprofen demonstrates the versatility and utility of this metal-free borylation. An exclusive monoselectivity was observed without a trace of diboration. Despite the possibility of forming a 5-membered boronated intermediate at the *ortho*-position, the selectively 6-membered intermediate paved the way for the formation of the *peri*-product, which was further supported by detailed computational investigation.

**KEYWORDS:** metal free, borylation, *peri*-functionalization, regioselective, amide



## INTRODUCTION

Over the last few decades, there has been an upsurge in carbon–boron bond formation among the synthetic research community.<sup>1–9</sup> Organo-boron reagents have become essential components for synthesizing natural products, drug molecules, pharmaceuticals, and advanced materials.<sup>10–13</sup> To date, among the different strategies applied to synthesize organo-boron reagents, the two most common methods are (a) cross-coupling and (b) transition metal (TM) catalyzed directed C–B bond formation *via* C–H bond activation.<sup>14–18</sup> Although these approaches have advantages due to their high regioselectivity, excellent yield, and functional group tolerance, limitations including the toxicity of certain transition metals and high cost have encouraged synthetic chemists to explore metal-free routes.<sup>19–24</sup>  $\text{BBr}_3$  is an effective borylating agent in this realm as it is highly reactive, available on a multigram scale, and cheaper than other common borylating reagents.<sup>25</sup>

Site-selective, metal-free electrophilic C–H borylation is accomplished by coordinating a heteroatom (*e.g.*, N, P, O, S) with  $\text{BBr}_3$ , generally forming a six-membered boronated metallacycle.<sup>26–39</sup> In 1993, Nicholson and coworkers reported the first example of a carbonyl-directed electrophilic C–H borylation reaction.<sup>40</sup> In recent times, Shi and coworkers reported a mild metal-free approach for the pivaloyl-directed C–H borylation of indoles selectively at the C4 and C7 positions.<sup>41</sup> In the same year, Ingleson and coworkers achieved *N*-acyl-directed C7 borylation of indoles (Scheme 1A).<sup>42</sup>

Further, they have extended this metal-free strategy for the *ortho*-borylation of *N*-pivaloyl- and *N*-benzoyl-protected anilines. Shi and Houk's groups disclosed a general protocol for the site-selective C2-borylation of pyrroles using  $\text{BBr}_3$  as a borylating agent.<sup>43</sup> Recently, Chatani and coworkers explored the pyrimidine-directed metal-free C–H borylation of 2-pyrimidylanilines.<sup>44</sup> Additionally, the Ji and coworkers reported *ortho*-borylation of toluene and thiobenzene by installing the pyridine and pyrazole-based directing group (Scheme 1B).<sup>45–47</sup> In 2022, Ingleson and coworkers extended the protocol for the *meta*-borylation of phenylacetic acids using an amino-pyridyl directing group approach; however, they were unable to achieve the *meta*-selective product.<sup>48</sup> Instead, they observed the usual amide-directed *ortho*-borylation, and the reaction's scope remained limited.

Notably, reported metal-free borylation reactions (*vide supra*) are mainly studied with electron-rich and heterocycle-based systems. However, due to inherent electron deficiency, aromatic electrophilic borylation of naphthamides under metal-free conditions remains unexplored. Since phenyl-

Received: July 23, 2024

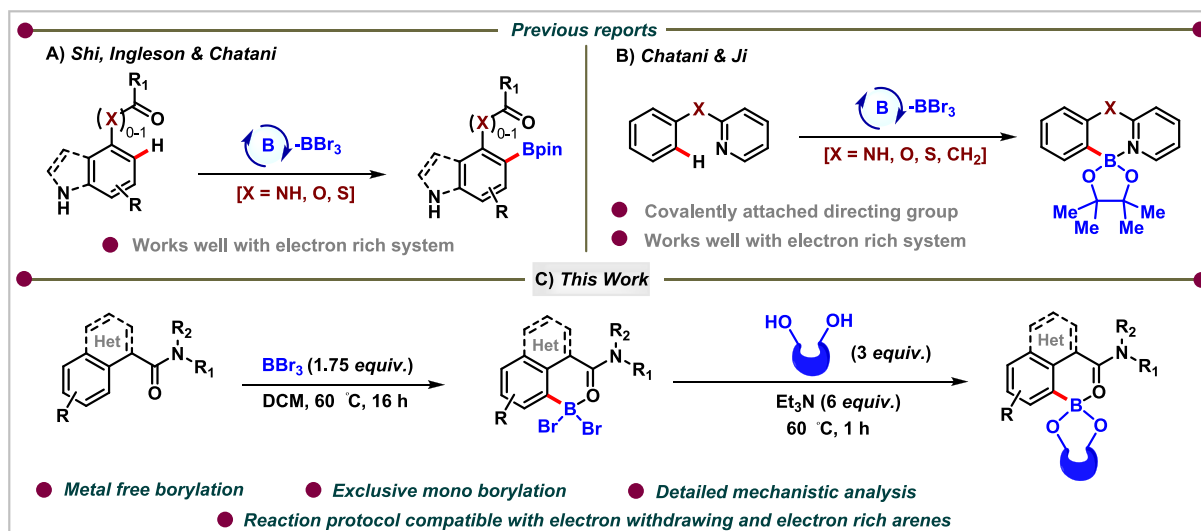
Revised: August 13, 2024

Accepted: August 14, 2024

Published: September 11, 2024



**Scheme 1. Previous Work: Regioselective Metal-free *ortho*-Borylation of (Hetero)arenes; Our Work: BBr<sub>3</sub>-Mediated Selective *peri*- and *ortho*-Borylation of Naphthamides and Phenylacetamides, Respectively**



acetamides and naphthamides are found in many natural products and drug molecules,<sup>49–53</sup> we aimed to develop a direct *ortho*- or *peri*-borylation of amides under mild and environmentally benign conditions. Herein, we report a facile methodology for metal-free C–H borylation of  $\alpha$ -naphthamides and phenylacetamides (Scheme 1C).

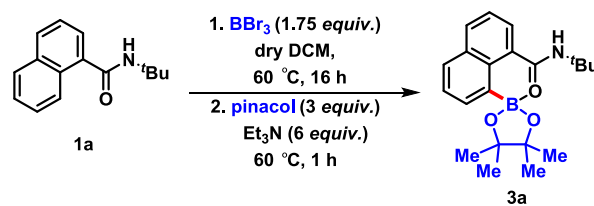
## RESULTS

### Optimization Details

To accomplish our objective of metal-free borylation of an electron-deficient system, we began our investigation with *N*-*tert*-butyl naphthamide **1a**. Keeping in mind the coordination ability of the electronegative oxygen atom toward a Lewis acid and the electropositive boron atom, we chose BBr<sub>3</sub> (1 equiv) as our primary borylating agent. The initial trial reaction of **1a** with BBr<sub>3</sub> in DCM solvent at room temperature did not give the desired product. We decided to increase the amount of BBr<sub>3</sub> to 1.25 equiv and the reaction temperature to 60 °C to check the formation of the desired borylated product **3a**. Interestingly, after 16 h of continuous stirring and quenching with pinacol (3 equiv) and Et<sub>3</sub>N (6 equiv), we observed the formation of the *peri*-borylated product **3a** in 51% yield (Table 1, entry 2). The structure of **3a** was further confirmed by detailed <sup>1</sup>H, <sup>13</sup>C, and <sup>11</sup>B NMR spectra. Despite the possibility of forming a 5-membered boronated intermediate at the *ortho*-position, the selectively 6-membered intermediate paved the way for the formation of the *peri*-product, which was further supported by detailed computational investigations (*vide infra*). Furthermore, no improvement in the product yield was observed upon elevating or decreasing the reaction temperature (Table 1, entries 3–5).

Changing the solvents from DCM to other chlorinated solvents, such as DCE, chloroform, and CCl<sub>4</sub>, decreased the reaction yield. No desired product was obtained when other nonpolar solvents (toluene, xylene, THF, *etc.*) were used (Table 1, entries 6 and 7). Notably, the amount of solvent played a crucial role in the reaction. When we increased the amount of BBr<sub>3</sub> to 1.75 equiv, **3a** was formed in 92% yield (Table 1, entry 10). A further increase in the amount of BBr<sub>3</sub> (2.5 equiv) produced a lower yield of **3a** (Table 1, entry 11).

**Table 1. Optimization of the Reaction Conditions for the Synthesis of **3a**<sup>a</sup>**



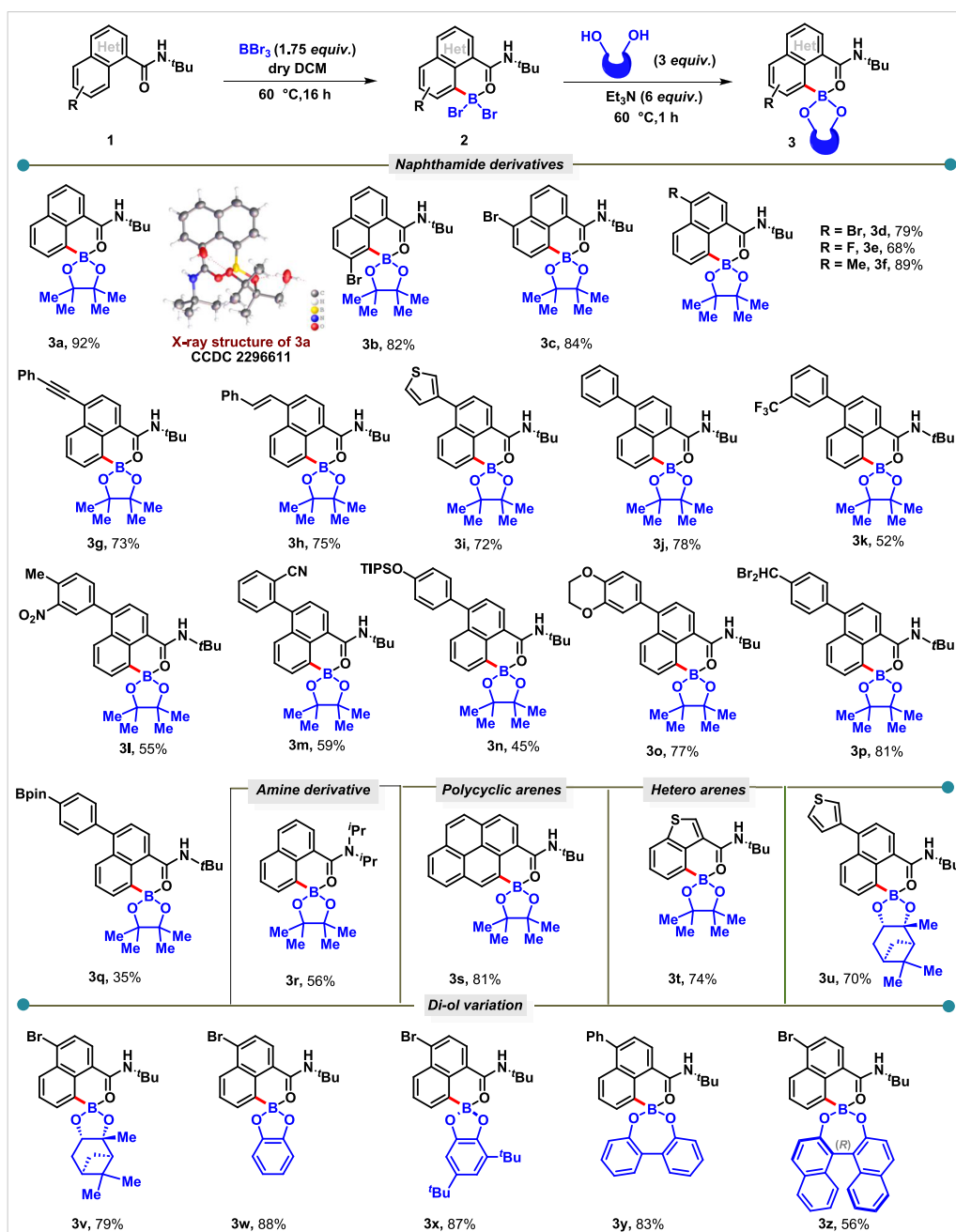
entry	variation from the "standard conditions"	yield % <sup>b</sup>
1	rt	NR
2	BBr <sub>3</sub> (1.25 equiv)	51%
3	40 °C	trace
4	50 °C	23%
5	70 °C	38%
6	DCE instead of DCM	27%
7	toluene instead of DCM	NR
8	DCM 1 mL (0.2 mmol)	30%
9	DCM 1.5 mL (0.2 mmol)	46%
10	none	92% (85%) <sup>c</sup>
11	BBr <sub>3</sub> (2.5 equiv)	43%
12	instead of BBr <sub>3</sub> , other borylated sources like BF <sub>3</sub> , BCl <sub>3</sub> , BI <sub>3</sub>	NR

<sup>a</sup>Standard reaction conditions: **1** (0.2 mmol), BBr<sub>3</sub> (1.75 equiv), dry DCM (1.5 mL), 60 °C, 16 h, then pinacol (3 equiv) and triethyl amine (6 equiv), 60 °C for 1 h. <sup>b</sup>NMR yield. <sup>c</sup>Isolated yield, NR: no reaction.

### Substrate Scope

With the final optimized conditions in hand, we expanded the substrate scope by varying different substituents on naphthamide derivatives (Scheme 2). The model substrate **1a** successfully transformed into the corresponding C8-borylated product (**3a**) in a 92% yield. A substituent at the C7 position was well-tolerated despite steric crowding, giving an 82% yield of the corresponding product **3b**. Both electron-donating and electron-withdrawing substituents are compatible with this protocol. Different positions of bromo-substituted naphthamides were successfully borylated (**3c**, 84%; **3d**, 79%). Moreover, *N*-(*tert*-butyl)-1-naphthamide with substituents at

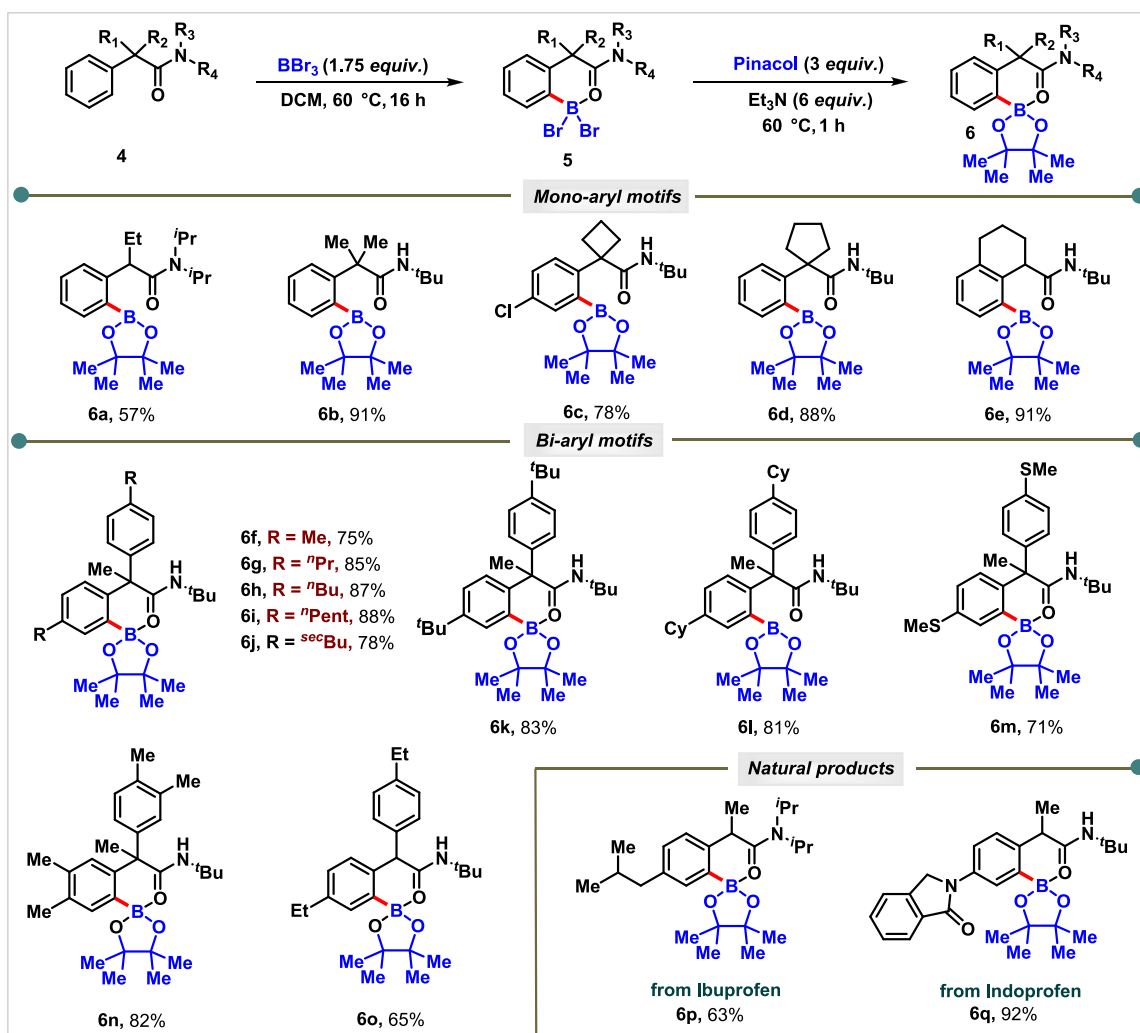
**Scheme 2. Substrate Scope of C8-Borylation of Naphthamides—Reaction Conditions: 1 (0.2 mmol), BBr<sub>3</sub> (1.75 equiv), Dry DCM (1.5 mL), 60°C, 16 h, Then Diol (3 equiv) and Triethyl Amine (6 equiv), 60°C for 1 h**



the 4-position (–F and –Me) underwent smooth borylation, yielding products **3e** (68%) and **3f** (89%), respectively. Interestingly, introducing styrene and phenylalkyne at the C4 position of the model substrate did not hinder the protocol. Instead of borylated products on the olefin or alkyne, we observed only C8-borylated products (**3g**, 73%; **3h**, 75%). Additionally, phenyl and heterocyclic-containing arenes, such as thiophene, are readily converted to the desired products (**3i**, 72%; **3j**, 78%). To assess the viability of this protocol, we introduced various functional groups (such as CF<sub>3</sub>, NO<sub>2</sub>, CN, OTIPS, and ether) into the C4-substituted phenyl ring. These modifications led to the formation of the corresponding C8-borylated products: **3k** (52%), **3l** (55%), **3m** (59%), **3n** (45%), and **3o** (77%). However, in the presence of aldehyde and

boronic acid functional groups in the arene ring, our protocol efficiently converts these to desired products **3p** (81%) and **3q** (35%). Simultaneously, the aldehyde group is converted to CHBr<sub>2</sub> and the boronic acid group is transformed to Bpin. Interestingly, *N,N*-diisopropyl-1-naphthamide is also well-tolerated in our methodology, leading to the desired product **3r** (56%). Changing the arene moiety from naphthalene to a polycyclic arene such as pyrene-1-carboxamide was readily converted into the corresponding product **3s** in 81% yield. This showcases, along with arenes, heteroarenes, which were also compatible with this reaction protocol. In this protocol, the C4-position of 3-substituted benzo-thiophene carboxamide is borylated, resulting in a 74% yield for compound **3t**. This methodology was also applied to bridged bicyclic diol, which

Scheme 3. Substrate Scope of *ortho*-Borylation of Phenyl Acetamide Derivatives—Reaction Conditions: **4** (0.2 mmol), BBr<sub>3</sub> (1.75 equiv), Dry DCM (1.5 mL), 60 °C, 16 h, Then Pinacol (3 equiv) and Triethyl Amine (6 equiv), 60 °C for 1 h



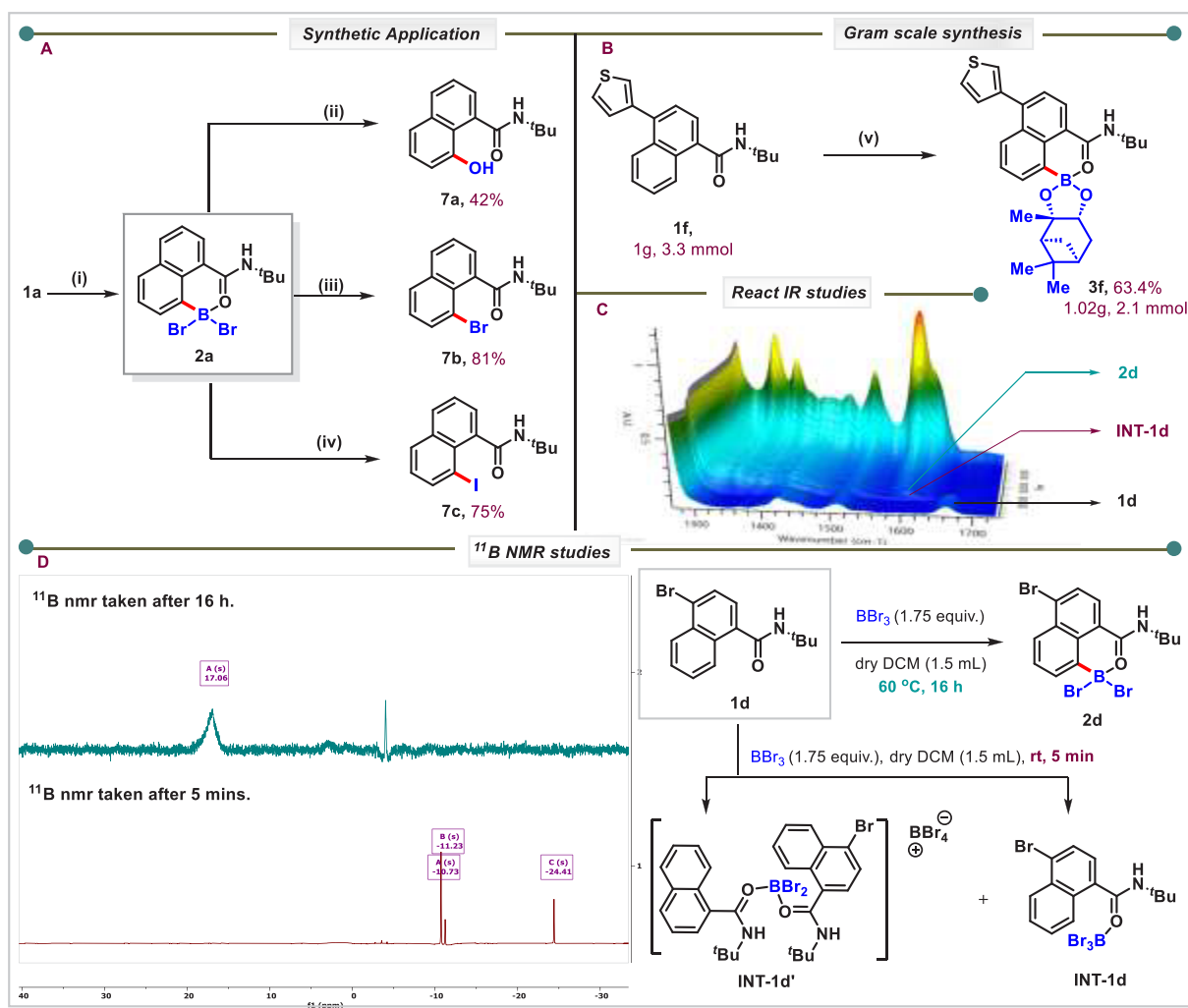
was converted to the bridged bicyclic borylating agents **3u** (70%) and **3v** (79%). The aromatic 1,2-diols such as catechol, 3,5-di-*tert*-butylbenzene-1,2-diol, [1,1'-biphenyl]-2,2'-diol, and (*R*)-BINOL were easily converted into their corresponding borylated products **3w** (88%), **3x** (87%), **3y** (83%), and **3z** (56%), respectively. For (*R*)-BINOL, the stereochemistry of the diol coupling partner remained intact during the product formation.

Further expanding the scope of this transformation, various phenyl acetamide derivatives with BBr<sub>3</sub> were explored, and the results were summarized in Scheme 3. Phenyl acetamide having  $\alpha$ -Et and  $\alpha, \alpha$ -di-Me substitutions were compatible with the optimized reaction conditions generating products in 57 and 91% yields, respectively. The presence of reactive  $\alpha$ -hydrogens, capable of tautomerizing in the presence of BBr<sub>3</sub>, also plays a role in reducing yields for **6a**. This also signifies that a quaternary center at the  $\alpha$ -position is more favorable for the reaction than a tertiary center. Also, the Thorpe–Ingold effect of two substituents pushed the phenyl group away, which ultimately helped in the formation of a six-membered boronated intermediate. Substrates having a smaller ring system (cyclobutane or cyclopentane) at the  $\alpha$ -position were also tolerated in this reaction protocol (**6c** and **6d**). Remarkably, 1,2,3,4-tetrahydronaphthalene-1-carboxamide

also reacted with BBr<sub>3</sub> and pinacol to afford the desired borylated product **6e** in a good yield (91%). The strategy showed good site selectivity and is even applicable to sterically congested C–H bonds, which certainly enriches the utility of this method. Treatment of biaryl-substrates with different alkyl variations (Me, Et, *t*-Bu, isobutyl, and even cyclohexyl) at the *para*-position of the phenyl rings also participated in the C–H borylation reaction (**6f–6l**, 75–88%). Instead with methyl deprotection on a *para*-substituted thiomethyl substrate, it gave the desired borylated product (**6m**). Furthermore, diphenyl acetic acid having disubstitutions at the phenyl ring was also susceptible to borylation under these reaction conditions (**6n**, 82%). Despite methyl substitution at the  $\alpha$  position of the diphenylacetamide derivatives, the substrate gave the desired product (**6o**, 65%) under the specified reaction conditions. As phenylacetic acids are commonly found drug motifs, late-stage borylation of these molecules will be an interesting opportunity to study their biological activities. Selective *ortho*-borylation of the drug scaffolds ibuprofen (**6p**) and indoprofen (**6q**) further demonstrates the synthetic potential of this strategy.

To assess the practicality of this method, a gram-scale borylation of **1f** was performed under standard reaction conditions without a notable decrease in yield (Scheme 4B).

**Scheme 4.** (A) Synthetic Applications of Metal-free Borylation—Reaction Conditions: (i)  $\text{BBr}_3$  (1.75 equiv), DCM,  $60^\circ\text{C}$ , 16 h; (ii)  $\text{NaBO}_3 \cdot 4\text{H}_2\text{O}$  (0.6 mmol), THF/ $\text{H}_2\text{O}$  (4:1), rt, 6 h; (iii) Selectfluor (0.4 mmol), TBAB (2.2 equiv),  $\text{CH}_3\text{CN}/\text{H}_2\text{O}$  (1:1), rt, 2 h Then  $\text{CH}_3\text{CN}/\text{H}_2\text{O}$ ,  $60^\circ\text{C}$ , 12 h; (iv) Selectfluor (0.4 mmol), KI (2.2 equiv),  $\text{CH}_3\text{CN}/\text{H}_2\text{O}$  (1:1), rt, 2 h Then  $\text{CH}_3\text{CN}/\text{H}_2\text{O}$ ,  $60^\circ\text{C}$ , 12 h; (B) Gram Scale Synthesis—Reaction Conditions: (v) **1** (3.3 mmol),  $\text{BBr}_3$  (1.75 equiv), Dry DCM (10 mL),  $60^\circ\text{C}$ , 16 h, Then Diol (3 equiv) and Triethyl Amine (6 equiv),  $60^\circ\text{C}$  for 1 h; (C) React IR Study; and (D)  $^{11}\text{B}$  NMR Study



Excess  $\text{BBr}_3$  (1.75 equiv) is required to complete the reaction, as it acts as both the borylating agent and bromide abstractor. The resulting C–B bonds formed in the product could then be utilized in various downstream transformations. For example, treating **2a** with  $\text{NaBO}_3 \cdot 4\text{H}_2\text{O}$  led to the formation of hydroxylation product **7a**.<sup>54</sup> Moreover, the bromination and iodination of **2a** using TBAB and KI as stoichiometric reagents provided bromo- and iodo-substituted naphthamide **7b** and **7c**, respectively (Scheme 4A).<sup>55,56</sup>

The react IR spectroscopic experiment elucidated the intermediate involved in this metal-free borylation protocol, and the course of the reaction was observed from the characteristic IR bands. The reaction was performed using 4-bromo-*N*-(*tert*-butyl)-1-naphthamide (**1d**) and  $\text{BBr}_3$ . As shown in Scheme 4, when  $\text{BBr}_3$  was added to the solution of **1d**, the peak corresponding to  $1663\text{ cm}^{-1}$  disappeared instantly, and a new INT-1d ( $1605\text{ cm}^{-1}$ ) was formed. In the meantime, INT-1d was consumed to form the desired dibromo product **2d** ( $1590\text{ cm}^{-1}$ ). This experiment signified that the complexation of **1d** with  $\text{BBr}_3$  was a fast step, and the process from INT-1d to **2d** is slow and considered a rate-determining step. Further,

*in situ*  $^{11}\text{B}$  NMR studies were performed, and the experiment results were depicted in Scheme 4D.

Initially, the reaction of 4-bromo-*N*-(*tert*-butyl)-1-naphthamide (**1d**) (1 equiv) with  $\text{BBr}_3$  (1.75 equiv) in dry DCM without any additive for only 5 min at room temperature produced the carbonyl oxygen-coordinated  $\text{BBr}_3$  adduct. The peak at  $-10.73\text{ ppm}$  in  $^{11}\text{B}$  NMR corresponds to INT-1d. At the same time, another adducts formed INT-1d', and peaks at  $-11.23$  and  $-24.41\text{ ppm}$  could be assigned to the borenium intermediate (INT-1d'). When the reaction was carried out at  $60^\circ\text{C}$  for 16 h,  $^{11}\text{B}$  NMR of the reaction mixture resulted in two new peaks at  $17.08\text{ ppm}$ , corresponding to **2d**.

### Computational Study

To unravel the origin of regioselectivity and gain a deeper understanding of the mechanism, we performed density functional theory (DFT) calculations on the model reaction of *N*-*tert*-butyl naphthamide (**1**) and  $\text{BBr}_3$  (Figure 1) at the B3LYP/def2-TZVP, SMD( $\text{CH}_2\text{Cl}_2$ )/B3LYP/def2-SVP level of theory.<sup>57–63</sup> In the first step of the reaction, the complexation of **1** and  $\text{BBr}_3$  occurs to form an exoergic adduct **2** ( $\Delta G = -8.5\text{ kcal mol}^{-1}$ , relative to **1**). Subsequently,

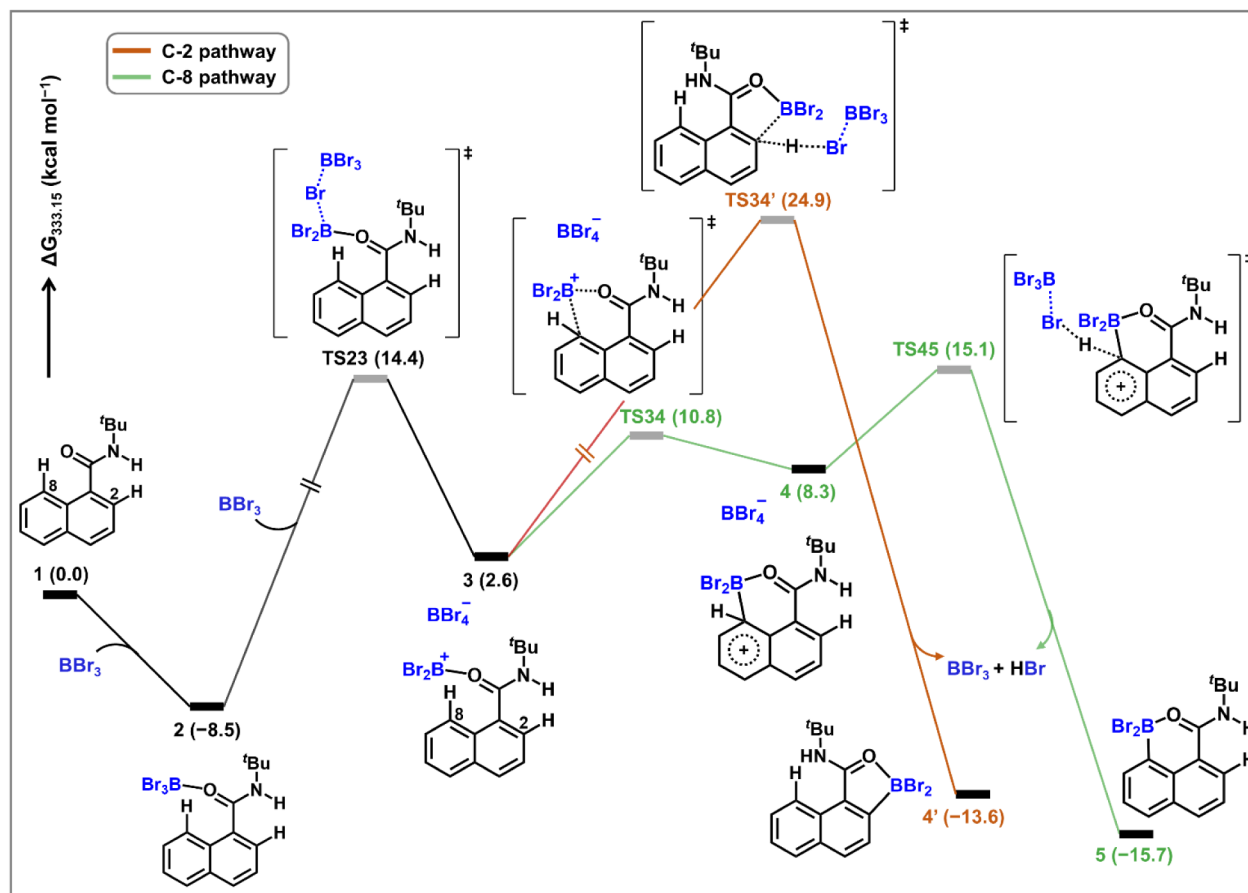


**Figure 1.** Mechanistic pathway for the metal-free borylation of  $\alpha$ -naphthamide. The numbers in parentheses are Gibbs free energies (in kcal mol<sup>-1</sup>).

bromine transfer from intermediate 2 to another BBr<sub>3</sub> molecule occurs *via* transition state TS23 with an activation barrier of 22.9 kcal mol<sup>-1</sup> (relative to 2) to form boronated species 3. The next step in 3 is intramolecular electrophilic substitution, which can proceed at the C2 and C8 positions. Electrophilic attack at the C2 position and deprotonation by BBr<sub>4</sub><sup>-</sup> occurs through a concerted transition state TS34' with an overall activation barrier of 33.4 kcal mol<sup>-1</sup> (relative to 2) to produce the C2-borylated product. Similarly, the electrophilic attack at the C8 position followed by deprotonation by BBr<sub>4</sub><sup>-</sup> proceeds *via* consecutive transition states TS34 and TS45 with activation barriers of 19.3 and 23.6 kcal mol<sup>-1</sup> (relative to 2), respectively, to form the C8-borylated product.

Thus, the overall activation barrier required to generate a C8-borylated product is 23.6 kcal mol<sup>-1</sup> which is favorable over the C-2 pathway by 9.8 kcal mol<sup>-1</sup> (Figure 1). This observation is in line with the experimental findings that C2-borylated products are not observed. To comprehend the origin of regioselectivity, we performed distortion/interaction analysis (DIA) for the transition states TS34' and TS45 (Figure 2). In DIA, we divided TS34' and TS45 into HBr, BBr<sub>3</sub>, and pro fragments and calculated the difference in distortion ( $\Delta\Delta E_{\text{dis}}$ ) and interaction ( $\Delta\Delta E_{\text{int}}$ ) energies. The DIA study reveals that the HBr, BBr<sub>3</sub>, and pro components in TS34 show a higher distortion of 5.8, 3.0, and 5.7 kcal mol<sup>-1</sup> than TS45. Thus, in TS34', distortion energy ( $\Delta\Delta E_{\text{dis}}$ ) is 14.5 kcal mol<sup>-1</sup> higher than TS45, while interaction energy favors TS34' by 4.5 kcal mol<sup>-1</sup>. Therefore, the distortion energy in

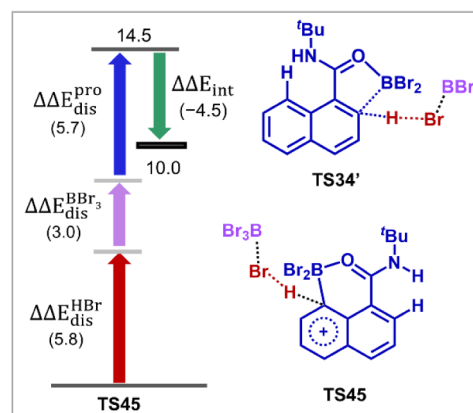


**Figure 2.** Distortion/interaction analysis for the transition states TS34' and TS45.

the fragments plays a dominant role in determining the regioselectivity of the products.

Next, we determined the mechanistic route for the borylation reaction of phenyl-acetamide substrates. The *N*-(*tert*-butyl)-2-methyl-2-phenylpropanamide (A) compound was chosen as a model substrate for phenyl acetamide. Initially, the complexation of A and BBr<sub>3</sub> gives stable adduct B ( $\Delta G = -3.7$  kcal mol<sup>-1</sup>, relative to A, Figure 3). In the next step, adduct B undergoes bromine transfer to the second molecule of BBr<sub>3</sub> through a transition state TSBC with an activation barrier of 23.8 kcal mol<sup>-1</sup> (relative to 4b) to produce

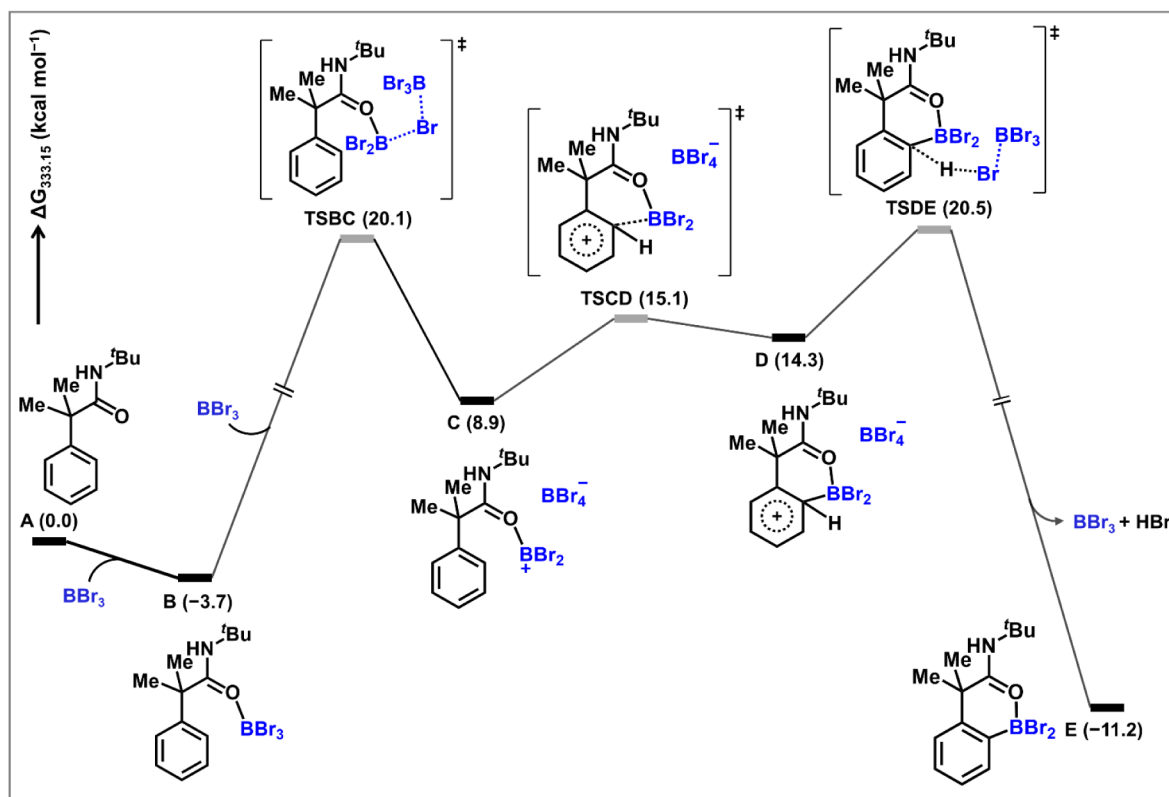


**Figure 3.** Mechanistic pathway for the metal-free borylation of phenyl acetamide. The numbers in parentheses are Gibbs free energies (in kcal mol<sup>-1</sup>) relative to those of A.

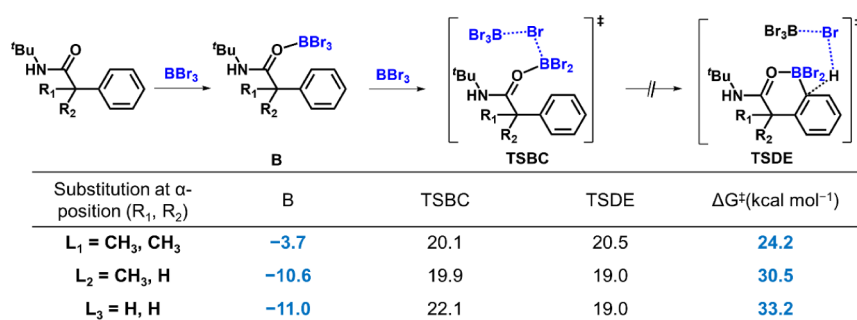


**Figure 4.** Reaction energetics of the borylation reaction of phenyl acetamide with different substituents at the  $\alpha$ -position.

a boronated intermediate C. Intramolecular electrophilic attack at the C-2 position of C proceeds *via* TSBCD requiring an energy barrier of 6.2 kcal mol<sup>-1</sup> (relative to C) to generate a Wheland intermediate D. Subsequently, D furnishes product E through transition state TSDE with an activation barrier of 6.2 kcal mol<sup>-1</sup> (relative to D). Thus, the overall energy barrier for the borylation reaction of A to generate product E is 24.2 kcal mol<sup>-1</sup> (B  $\rightarrow$  TSDE).

The substituent attached to the  $\alpha$ -position of phenyl acetamide substrates influences the reactivity toward the borylation reaction. The substrates with bulkier groups at the  $\alpha$ -position give the desired product efficiently. To understand the reactivity difference, we calculated different  $R_1$  and  $R_2$  substitutions of phenyl acetamide (Figure 4). In the case of  $L_1$  ( $R_1 = \text{CH}_3$  and  $R_2 = \text{CH}_3$ ), the initial complexation with BBr<sub>3</sub> results in the intermediate B ( $\Delta G = -3.7$  kcal mol<sup>-1</sup>, relative to A). However, with  $L_2$  ( $R_1 = \text{CH}_3$  and  $R_2 = \text{H}$ ), the

complexation provides a surprisingly stable amide–BBr<sub>3</sub> complex ( $\Delta G = -10.6$  kcal mol<sup>-1</sup>).

A similar stability of the amide–BBr<sub>3</sub> complex ( $\Delta G = -11.0$  kcal mol<sup>-1</sup>) is observed with  $L_3$  ( $R_1 = \text{H}$  and  $R_2 = \text{H}$ ). To determine the energetics of the reaction, we computed the overall activation barrier by determining transition states TSBC and TSDE with different  $R_1$  and  $R_2$  substituents. In the case of  $L_1$ , the overall energy barrier for the reaction is 24.2 kcal mol<sup>-1</sup>. However, with  $L_2$  and  $L_3$ , despite having similar energetics for the transition states, the overall energy barrier reaches 30.5 and 33.2 kcal mol<sup>-1</sup>, respectively. Thus, it can be inferred that the relative stability of amide–BBr<sub>3</sub> is the determining factor for reaction energetics as amide–BBr<sub>3</sub> is a turnover-determining intermediate.

To comprehend the difference in the relative stability of the amide–BBr<sub>3</sub> complex in all three cases, we performed DIA in which intermediate B is divided into amide and BBr<sub>3</sub> fragments. In this analysis, we computed the distortion and

interaction energy occurring during the interaction of amide and  $\text{BBr}_3$ . On moving from  $\text{L}_1$  to  $\text{L}_3$ , the  $\text{BBr}_3$  fragment shows distortion energy of  $33.5 \text{ kcal mol}^{-1}$  in  $\text{L}_1$ ,  $30.7 \text{ kcal mol}^{-1}$  in  $\text{L}_2$ , and  $29.6 \text{ kcal mol}^{-1}$  in  $\text{L}_3$ . The two methyl groups at the  $\alpha$ -position show steric repulsion with the bromine atoms of  $\text{BBr}_3$ , resulting in large distortion energy in  $\text{L}_1$  as compared to  $\text{L}_2$  and  $\text{L}_3$ . The interaction energies between the amide and  $\text{BBr}_3$  fragments in  $\text{L}_1$ ,  $\text{L}_2$ , and  $\text{L}_3$  are  $-56.0$ ,  $-59.4$ , and  $-58.9 \text{ kcal mol}^{-1}$ , respectively (Figure 5). Thus, in the case of  $\text{L}_1$ , the

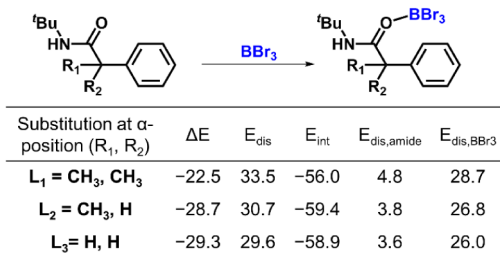


**Figure 5.** Distortion/interaction analysis for the intermediates **A** and **B** produced in borylation of phenyl acetamide with different  $\text{R}_1$  and  $\text{R}_2$  substituents at the  $\alpha$ -position.

more distortion and less interaction energies provide the amide– $\text{BBr}_3$  complex stability to only  $-22.5 \text{ kcal mol}^{-1}$  ( $\Delta E$ , relative to amide). However, in  $\text{L}_2$  and  $\text{L}_3$ , the complex is more stabilized with relative electronic energies of  $-28.7$  and  $-29.3 \text{ kcal mol}^{-1}$ , respectively. So, it can be inferred that bulky groups hinder the formation of a stable amide– $\text{BBr}_3$  complex, and thus, the overall reaction energy barrier remains affordable under the present reaction conditions.

In order to understand the effect of substitution at the nitrogen of the amide, we replaced the  $^t\text{Bu}$  ( $\text{L}_4$ ) group with Me ( $\text{L}_5$ ), and H ( $\text{L}_6$ ) groups. The relative stability of the amide– $\text{BBr}_3$  complex in  $\text{L}_4$ ,  $\text{L}_5$ , and  $\text{L}_6$  is  $-3.7$ ,  $-6.0$ , and  $-10.1 \text{ kcal mol}^{-1}$ , respectively (Figure 6). The overall energy barrier is  $24.2 \text{ kcal mol}^{-1}$  for  $\text{L}_4$ ,  $28.6 \text{ kcal mol}^{-1}$  for  $\text{L}_5$ , and  $35.4 \text{ kcal mol}^{-1}$  for  $\text{L}_6$ . It is evident that a bulkier substituent like  $^t\text{Bu}$  does not provide stability to the amide– $\text{BBr}_3$  complex; however, in the case of Me and H, the complex is more stabilized which results in a higher overall energy barrier for the reaction.

To understand the difference in relative stability of the amide– $\text{BBr}_3$  complex, we performed DIA in which intermediate **B** is divided into amide and  $\text{BBr}_3$  fragments. The relative electronic energies of **B** (relative to the respective amide) in  $\text{L}_4$ ,  $\text{L}_5$ , and  $\text{L}_6$  are  $-22.5$ ,  $-24.8$ , and  $-28.3 \text{ kcal mol}^{-1}$ , respectively (Figure 7). In the case of  $\text{L}_5$  and  $\text{L}_6$ , the

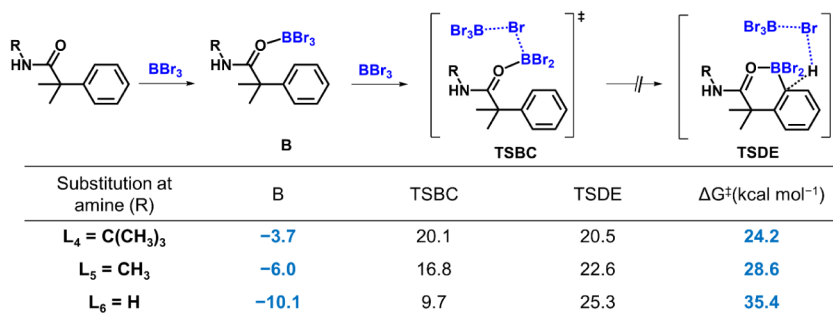


**Figure 6.** Reaction energetics of borylation of phenyl acetamide with different substituents at the nitrogen of amide.

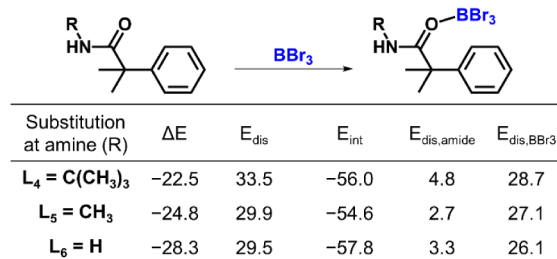


**Figure 7.** Distortion/interaction analysis for the reaction between phenyl acetamide and  $\text{BBr}_3$  to form **B** with different substitutions at amine.

total distortion energy for the complexation of  $\text{BBr}_3$  with amide is almost the same ( $29.9$  and  $29.5 \text{ kcal mol}^{-1}$ ), whereas in  $\text{L}_4$  it is  $33.5 \text{ kcal mol}^{-1}$ . Moreover, the interaction energies between the amide and  $\text{BBr}_3$  fragments in  $\text{L}_4$ ,  $\text{L}_5$ , and  $\text{L}_6$  are  $-56.0$ ,  $-54.6$ , and  $-57.8 \text{ kcal mol}^{-1}$ , respectively. Hence, in  $\text{L}_4$ , higher distortion and lesser interaction energies compared to those in  $\text{L}_5$  and  $\text{L}_6$  destabilize intermediate **B** and consequently decrease the overall activation barrier for the reaction. In  $\text{L}_5$  and  $\text{L}_6$ , lesser distortion and similar interaction energies in comparison with  $\text{L}_4$  stabilize intermediate **B** and in return, the overall activation barrier increases to  $28.6 \text{ kcal mol}^{-1}$  (in  $\text{L}_5$ ) and  $35.4 \text{ kcal mol}^{-1}$  (in  $\text{L}_6$ ).

In brief, the computational investigation of the borylation of  $\alpha$ -naphthamides offers fruitful insights into selectivity for the C8 position over the C2 position. Shi and coworkers in their DFT calculation demonstrated that the C–H borylation of indoles selectively forms the C7 product over the C2 product.<sup>41</sup> The authors further depicted that the regioselectivity of the reaction might be due to the larger distortion energy suffered by the transition state leading to the C2 product. In 2021, Shi and coworkers showcased the mechanistic routes of the C–H borylation of pyrroles for the selective formation of the C2 product over the C5 product.<sup>43</sup> In this present work, we utilized DIA to comprehend the regioselectivity and revealed that distortion energy in the fragments plays a dominant role in determining the selectivity to the C8 product over the C2 product. Chatani and coworkers performed the computation over metal-free ortho C–H borylation of benzaldehyde derivatives.<sup>32</sup> The authors revealed that the bulkier substituents attached to the imine substrate favor efficient formation of the product. Similarly, in the present work, the computations unveil that the overall activation barrier is affordable if the bulkier substituents at the nitrogen and the  $\alpha$ -position of phenyl acetamide are present.



## CONCLUSIONS

In summary, we developed a method for metal-free C–H borylation of  $\alpha$ -naphthamides and phenylacetic acid drugs. The proposed strategy showcased good functional group tolerance and high efficiency. Borylated compounds were produced under mild, convenient, and economical conditions with excellent yields and site exclusivity. Computational analysis reveals that the borylation of  $\alpha$ -naphthamide and phenyl acetamide proceeds with an overall activation barrier of 23.6 and 24.2 kcal mol<sup>-1</sup>, respectively. The distortion/interaction analysis further revealed that the bulky substituents at the  $\alpha$ -position and *N*-position of phenyl acetamide lower the overall activation barrier and thus favor the formation of the product under the present reaction conditions.

## EXPERIMENTAL SECTION

### General Procedure of Metal-Free Borylation of $\alpha$ -Naphthamides and Phenylacetic Acid Drug

An oven-dried screw cap reaction tube was charged with a magnetic stir bar and amide (0.2 mmol); then 1.2 mL of dry DCM was added. After adding DCM, BBr<sub>3</sub> (1.75 equiv) was added to the reaction tube. Then, the reaction mixture was stirred vigorously in a preheated oil bath at 60 °C. The reaction was carried out for 16 h, and after that, pinacol (3 equiv) and triethyl amine (6 equiv) were added to the same reaction pot. Again, the reaction mixture was heated in the same preheated oil bath for 1 h. Then, the reaction mixture was diluted with DCM, and the solvent was evaporated; the desired borylated product was isolated by column chromatography using silica gel (100–200 mesh size).

## ASSOCIATED CONTENT

### Supporting Information

The Supporting Information is available free of charge at <https://pubs.acs.org/doi/10.1021/jacsau.4c00660>.

Experimental procedures, analytical data (<sup>1</sup>H, <sup>13</sup>C NMR, <sup>11</sup>B NMR, HRMS), computational details and DFT-optimized structures (PDF)  
CIF/PLATON report (PDF)

## AUTHOR INFORMATION

### Corresponding Authors

**Puneet Gupta** – Computational Catalysis Center, Department of Chemistry, Indian Institute of Technology Roorkee, Roorkee, Uttarakhand 247667, India; Department of Chemistry, Faculty of Science Center for Sustainable Energy, Indian Institute of Technology Roorkee, Roorkee, Uttarakhand 247667, India; [orcid.org/0000-0002-3004-2936](https://orcid.org/0000-0002-3004-2936); Email: [puneet.gupta@cy.iitr.ac.in](mailto:puneet.gupta@cy.iitr.ac.in)

**Debabrata Maiti** – Department of Chemistry, Indian Institute of Technology Bombay, Mumbai 400076, India; [orcid.org/0000-0001-8353-1306](https://orcid.org/0000-0001-8353-1306); Email: [dmaiti@iitb.ac.in](mailto:dmaiti@iitb.ac.in)

### Authors

**Suman Maji** – Department of Chemistry, Indian Institute of Technology Bombay, Mumbai 400076, India

**Parveen Rawal** – Computational Catalysis Center, Department of Chemistry, Indian Institute of Technology Roorkee, Roorkee, Uttarakhand 247667, India; [orcid.org/0000-0002-3268-9020](https://orcid.org/0000-0002-3268-9020)

**Animesh Ghosh** – Department of Chemistry, Indian Institute of Technology Bombay, Mumbai 400076, India

**Karishma Pidiyar** – Department of Chemistry, Indian Institute of Technology Bombay, Mumbai 400076, India

**Shaeel A. Al-Thabaiti** – Department of Chemistry, Faculty of Science, King Abdulaziz University institution, Jeddah, 21589, Saudi Arabia

Complete contact information is available at:  
<https://pubs.acs.org/10.1021/jacsau.4c00660>

### Author Contributions

S.M. and D.M. conceived the concept. S.M., A.G., and K.P. performed the reactions and analyzed the products. S.M., A.G., K.P., and D.M. designed the control experiments and mechanistic pathway. P.R. and P.G. designed and performed the computational studies and analyzed the results. The manuscript was written with contributions from all authors. All authors have approved the final version of the manuscript.

### Notes

The authors declare no competing financial interest.

## ACKNOWLEDGMENTS

The Institutional Fund Project funded this research work under grant no. IFPIP: 312-130-1443. The authors gratefully acknowledge technical and financial support from the Ministry of Education and King Abdulaziz University, DSR, Jeddah, Saudi Arabia. P.R. thanks CSIR for the SRF fellowship (09/143(1001)/2019–EMR–I). P.G. acknowledges SERB (CRG/2021/000759) for financial support and National Supercomputing Mission (NSM) for providing computing resources of PARAM Ganga at IIT Roorkee, which is implemented by C–DAC and supported by the Ministry of Electronics and Information Technology (MeitY) and Department of Science and Technology (DST), Government of India.

## REFERENCES

- (1) Ishiyama, T.; Murata, M.; Miyaura, N. Palladium (0)-catalyzed cross-coupling reaction of alkoxydiboron with haloarenes: A direct procedure for arylboronic esters. *J. Org. Chem.* **1995**, *60*, 7508.
- (2) Ishiyama, T.; Takagi, J.; Hartwig, J. F.; Miyaura, N. A stoichiometric aromatic C–H borylation catalyzed by iridium (I)/2,2'-bipyridine complexes at room temperature. *Angew. Chem., Int. Ed.* **2002**, *41*, 3056.
- (3) Hata, H.; Yamaguchi, S.; Mori, G.; Nakazono, S.; Katoh, T.; Takatsu, K.; Hiroto, S.; Shinokubo, H.; Osuka, A. Regioselective Borylation of Porphyrins by C–H Bond Activation under Iridium Catalysis to Afford Useful Building Blocks for Porphyrin Assemblies. *Chem. - Asian J.* **2007**, *7*, 849.
- (4) Hartwig, J. F. Regioselectivity of the borylation of alkanes and arenes. *Chem. Soc. Rev.* **2011**, *40*, 1992.
- (5) Kuninobu, Y.; Ida, H.; Nishi, M.; Kanai, M. A meta-selective C–H borylation directed by a secondary interaction between ligand and substrate. *Nat. Chem.* **2015**, *7*, 712.
- (6) Lu, X.; Yoshigoe, Y.; Ida, H.; Nishi, M.; Kanai, M.; Kuninobu, Y. Hydrogen Bond-Accelerated meta-Selective C–H Borylation of Aromatic Compounds and Expression of Functional Group and Substrate Specificities. *ACS Catal.* **2019**, *9*, 1705.
- (7) Pandit, S.; Maiti, S.; Maiti, D. Noncovalent interactions in Ir-catalyzed remote C–H borylation: A recent update. *Org. Chem. Front.* **2021**, *8*, 4348.
- (8) Fontaine, F.; Desrosiers, V. Synthesis Boron Lewis Pair Mediated C–H Activation and Borylation. *Synthesis* **2021**, *53*, 4599.
- (9) Bisht, R.; Haldar, C.; Hassan, M. M.; Hoque, E. M. M.; Chaturvedi, J.; Chattopadhyay, B. Metal-catalysed C–H bond activation and borylation. *Chem. Soc. Rev.* **2022**, *51*, 5042.

- (10) Shiner, C. S.; Garner, C. M.; Haltiwanger, R. C. Synthesis and crystal structure of an optically active, internally coordinated alkylchloroborane. The boron-centered anomeric effect. *J. Am. Chem. Soc.* **1985**, *107*, 7167.
- (11) Kaur, P.; Khatik, G. L.; Nayak, S. K. A review on advances in organoborane-chemistry: Versatile tool in asymmetric synthesis. *Curr. Org. Synth* **2017**, *14*, 665.
- (12) Wilson, T. C.; Cailly, T.; Gouverneur, V. Boron reagents for divergent radiochemistry. *Chem. Soc. Rev.* **2018**, *47*, 6990.
- (13) Kalita, S. J.; Cheng, F.; Huang, Y. Y. Recent Advances of Applying Boron-Reagents in Asymmetric Total Syntheses of Natural Products and Bio-Active Molecules. *Adv. Syn. Catal.* **2020**, *362*, 2778.
- (14) Miyaura, N.; Suzuki, A. Palladium-catalyzed cross-coupling reactions of organoboron compounds. *Chem. Rev.* **1995**, *95*, 2457.
- (15) Murata, M.; Oyama, T.; Watanabe, S.; Masuda, Y. Palladium-catalyzed borylation of aryl halides or triflates with dialkoxyborane: A novel and facile synthetic route to arylboronates. *J. Org. Chem.* **2000**, *65*, 164.
- (16) Yamamoto, Y.; Fujikawa, R.; Umamoto, T.; Miyaura, N. Iridium-catalyzed hydroboration of alkenes with pinacolborane. *Tetrahedron* **2004**, *60*, 10695.
- (17) Dudnik, A. S.; Fu, G. C. Nickel-catalyzed coupling reactions of alkyl electrophiles, including unactivated tertiary halides, to generate carbon–boron bonds. *J. Am. Chem. Soc.* **2012**, *134*, 10693.
- (18) Tobisu, M.; Kinuta, H.; Kita, Y.; Rémond, E.; Chatani, N. Rhodium (I)-catalyzed borylation of nitriles through the cleavage of carbon–cyano bonds. *J. Am. Chem. Soc.* **2012**, *134*, 115.
- (19) Shamsabadi, A.; Chudasama, V. Recent advances in metal-free aerobic C–H activation. *Org. Biomol. Chem.* **2019**, *17*, 2865.
- (20) Lva, J.; Zhaoc, B.; Hana, Y.; Yuan, Y.; Shi, Z. Metal-free cascade boron–heteroatom addition and alkylation with diazo compounds. *Chin. Chem. Lett.* **2021**, *32*, 691.
- (21) Paul, N.; Patra, T.; Maiti, D. Recent developments in hydrocyanation and decyanative functionalization reaction. *Asian J. Org. Chem.* **2021**, *10*, No. e202100591.
- (22) Hazra, S.; Mahato, S.; Das, K. K.; Panda, S. Transition-Metal-Free Heterocyclic Carbon-Boron Bond Formation. *Chem.-Eur. J.* **2022**, *28*, No. e202200556.
- (23) Grover, J.; Prakash, G.; Teja, C.; Lahiri, G. K.; Maiti, D. Metal-free photoinduced hydrogen atom transfers assisted C (sp<sup>3</sup>)–H thioarylation. *Green Chem.* **2023**, *25*, 3431.
- (24) Roy, S.; Panja, S.; Sahoo, S. R.; Chatterjee, S.; Maiti, D. Enroute sustainability: Metal free C–H bond functionalisation. *Chem. Soc. Rev.* **2023**, *52*, 2391.
- (25) Tanaka, S.; Saito, Y.; Yamamoto, T.; Hattori, T. Electrophilic Borylation of Terminal Alkenes with BBr<sub>3</sub>/2,6-Disubstituted Pyridines. *Org. Lett.* **2018**, *20*, 1828.
- (26) Ishida, N.; Moriya, T.; Goya, T.; Murakami, M. Synthesis of Pyridine–Borane Complexes via Electrophilic Aromatic Borylation. *J. Org. Chem.* **2010**, *75*, 8709.
- (27) Iqbal, S. A.; Pahl, J.; Yuan, K.; Ingleson, M. J. Intramolecular (directed) electrophilic C–H borylation. *Chem. Soc. Rev.* **2020**, *49*, 4564.
- (28) Li, Y.; Wu, X. F. Direct C–H bond borylation of (hetero)arenes: Evolution from noble metal to metal free. *Angew. Chem., Int. Ed.* **2020**, *59*, 1770.
- (29) Rej, S.; Chatani, N. Regioselective Transition-Metal-Free C(sp<sup>2</sup>)-H Borylation: A Subject of Practical and Ongoing Interest in Synthetic Organic Chemistry. *Angew. Chem., Int. Ed.* **2021**, *12*, 1144.
- (30) Chen, C. H.; Zheng, W. H. Planar chiral B–N heteroarenes based on [2.2] paracyclophane as circularly polarized luminescence emitters. *Org. Lett.* **2021**, *23*, 5554.
- (31) Rej, S.; Chatani, N. Transient Imine as a Directing Group for the Metal-Free o-C–H Borylation of Benzaldehydes. *J. Am. Chem. Soc.* **2021**, *143*, 2920.
- (32) Yamazaki, K.; Rej, S.; Ano, Y.; Chatani, N. Origin of the Enhanced Reactivity in the ortho C–H Borylation of Benzaldehydes with BBr<sub>3</sub>. *Org. Lett.* **2022**, *24*, 213.
- (33) Sadek, O.; Le Gac, A.; Hidalgo, N.; Ladeira, S. M.; Miqueu, K.; Bouhadir, G.; Bourissou, D. Metal-Free Phosphorus-Directed Borylation of C(sp<sup>2</sup>)–H Bonds. *Angew. Chem., Int. Ed.* **2022**, *61*, No. e202110102.
- (34) Berionni, G. Regioselective Transition-Metal-Free Arene C–H Borylations: From Directing Groups to Borylation Template Reagents. *Angew. Chem., Int. Ed.* **2022**, *61*, No. e202210284.
- (35) Iqbal, S. A.; Uzelac, M.; Nawaz, I.; Wang, Z.; Jones, T. H.; Yuan, K.; Millet, C. R. P.; Nichol, G. S.; Chotana, G. A.; Ingleson, M. J. Amides as Modifiable Directing Groups in Electro-philic Borylation. *Chem. Sci.* **2023**, *14*, 3865.
- (36) Wang, T.; Wang, Z. J.; Wang, M.; Wu, L.; Fang, X.; Liang, Y.; Lv, J.; Shi, Z. Metal-Free Stereoconvergent C–H Borylation of Enamides. *Angew. Chem., Int. Ed.* **2023**, *62*, No. e202313205.
- (37) Yang, C. H. BX<sub>3</sub>-mediated borylation for the synthesis of organoboron compounds. *Org. Chem. Front.* **2023**, *10*, 6010.
- (38) Lv, J.; Liang, Y.; Ouyang, Y.; Zhang, H. Metal-Free ortho C–H Borylation of Thiobenzamides. *Org. Lett.* **2024**, *26*, 3709.
- (39) Chen, W.; Jiatao, X.; Huang, J.; Zhou, L.; Wu, G. Chemoselective C–H Hydroxylation and Borylation of N-Phenylbenzamide using BBr<sub>3</sub>. *Org. Lett.* **2024**, *26*, 4631.
- (40) Arcus, V. L.; Main, L.; Nicholson, B. K. ortho-Directed electrophilic boronation of a benzyl ketone: The preparation, X-ray crystal structure, and some reactions of 4-ethyl-1-hydroxy-3-(4-hydroxyphenyl)-2-oxa-1-boranaphthalene. *J. Organomet. Chem.* **1993**, *460*, 139.
- (41) Lv, J.; Chen, X.; Xue, X.-S.; Zhao, B.; Liang, Y.; Wang, M.; Jin, L.; Yuan, Y.; Han, Y.; Zhao, Y.; Lu, Y.; Zhao, J.; Sun, W.-Y.; Houk, K. N.; Shi, Z. Metal-free directed sp<sup>2</sup>-C–H borylation. *Nature* **2019**, *575*, 336.
- (42) Iqbal, S. A.; Cid, J.; Procter, R. J.; Uzelac, M.; Yuan, K.; Ingleson, M. J. Acyl-Directed ortho-Borylation of Anilines and C7 Borylation of Indoles using just BBr<sub>3</sub>. *Angew. Chem., Int. Ed.* **2019**, *58*, 15381.
- (43) Wang, Z.-J.; Chen, X.; Wu, L.; Wong, J. J.; Liang, Y.; Zhao, Y.; Houk, K. N.; Shi, Z. Metal-Free Directed C–H Borylation of Pyrroles. *Angew. Chem., Int. Ed.* **2021**, *60*, 8500.
- (44) Rej, S.; Das, A.; Chatani, N. Pyrimidine-directed metal-free C–H borylation of 2-pyrimidylanilines: A useful process for tetra-coordinated triarylborane synthesis. *Chem. Sci.* **2021**, *12*, 11447.
- (45) Xua, X.; Wanga, S.; Chena, L.; Panga, B.; Ma, T.; Ji, Y. Metal-free directed C–H borylation of 2-(N-methylanilino)-5-fluoropyridines and 2-benzyl-5-fluoropyridines. *Chin. Chem. Lett.* **2022**, *33*, 2005.
- (46) Wu, G.; Pang, B.; Wang, Y.; Yan, L.; Chen, L.; Ma, T.; Ji, Y. Metal-Free ortho-Selective C–H Borylation of 2-Phenylthiopyridines Using BBr<sub>3</sub>. *J. Org. Chem.* **2021**, *86*, 5933.
- (47) Wu, G.; Xu, X.; Wang, S.; Chen, L.; Wang, B.; Ma, T.; Ji, Y. Metal-free directed C–H borylation of 2-(N-methylanilino)-5-fluoropyridines and 2-benzyl-5-fluoropyridines. *Chin. Chem. Lett.* **2021**, *9*, 81.
- (48) Iqbal, S. A.; Millet, C. R. P.; Pahl, J.; Yuan, K.; Ingleson, M. J. Amides as modifiable directing groups in electrophilic borylation. *Chem. Sci.* **2023**, *14*, 3865–3872.
- (49) Ibrahim, S. R. M.; Mohamed, G. A. Naturally occurring naphthalenes: Chemistry, biosynthesis, structural elucidation, and biological activities. *Phytochem. Rev.* **2016**, *15*, 279.
- (50) Mehndiratta, S.; Chen, M. C.; Chao, Y. H.; Lee, C. H.; Liou, J. P.; Lai, M. J.; Lee, H. Y. J. Effect of 3-substitution of quinolinehydroxamic acids on selectivity of histone deacetylase isoforms. *Enzyme Inhib. Med. Chem.* **2021**, *36*, 74.
- (51) Maji, S.; Pradhan, S.; Pidiyara, K.; Maiti, S.; Al-Thabaiti, S. A.; Maiti, D. Palladium-Catalysed Amide-Directed Ligand Free C8-Olefination of 1-Naphthamides for the Synthesis of 2,3-Dihydro-1H-Benzo[de]isoquinolin-1-ones. *Adv. Synth. Catal.* **2023**, *366*, 838–843.
- (52) Devi, N.; Rawal, R. K.; Singh, V. Diversity-oriented synthesis of fused-imidazole derivatives via Groebke–Blackburn–Bienayme reaction: A review. *Tetrahedron* **2015**, *71*, 183.

(53) Makar, S.; Saha, T.; Singh, S. K. Naphthalene a versatile platform in medicinal chemistry: Sky-high perspective. *Eur. J. Med. Chem.* **2019**, *161*, 252–276.

(54) Lv, J.; Zhao, B.; Yuan, Y.; Han, Y.; Shi, Z. Boron-mediated directed aromatic C–H hydroxylation. *Nat. Commun.* **2020**, *11*, 1316.

(55) Shinde, G. H.; Ghotekar, G. S.; Amombo Noa, F. M.; Öhrström, L.; Norrby, P.-O.; Sundén, H. Regioselective orthohalogenation of N-aryl amides and ureas via oxidative halodeboronation: Harnessing boron reactivity for efficient C-halogen installation. *Chem. Sci.* **2023**, *14*, 13429.

(56) Shinde, G. H.; Sundén, H. Boron-Mediated Regioselective Aromatic C–H Functionalization via an Aryl BF<sub>2</sub> Complex. *H. Chem.-Eur. J.* **2022**, *29*, No. e2022035.

(57) Neese, F. Wiley Interdiscip. *Rev. Comput. Mol. Sci.* **2012**, *2*, 73.

(58) Lee, C.; Yang, W.; Parr, R. G. Development of the Colle-Salvetti correlation-energy formula into a functional of the electron density. *Phys. Rev. B* **1988**, *37*, 785.

(59) Becke, A. D. Density-functional thermochemistry. I. The effect of the exchange-only gradient correction. *J. Chem. Phys.* **1993**, *98*, 5648.

(60) Weigend, F.; Ahlrichs, R. Balanced basis sets of split valences, triple zeta valence and quadruple zeta valence quality for H to Rn: Design and assessment of accuracy. *Phys. Chem. Chem. Phys.* **2005**, *7*, 3297.

(61) Neese, F.; Wennmohs, F.; Hansen, A.; Becker, U. Efficient, approximate and parallel Hartree–Fock and hybrid DFT calculations. A ‘chain-of-spheres’ algorithm for the Hartree–Fock exchange. *Chem. Phys.* **2009**, *356*, 98.

(62) Grimme, S.; Ehrlich, S.; Goerigk, L. Effect of the damping function in dispersion corrected density functional theory. *J. Comput. Chem.* **2011**, *32*, 1456.

(63) Marenich, A. V.; Cramer, C. J.; Truhlar, D. G. Universal Solvation Model Based on Solute Electron Density and on a Continuum Model of the Solvent Defined by the Bulk Dielectric Constant and Atomic Surface Tensions. *J. Phys. Chem. B* **2009**, *113*, 6378.